$Fe(CO)_5$ and be a heterogeneous catalyst if the solvent does not attact the $Fe(CO)_5$. The surface interactions between the metal carbonyl and the zeolite are quite complex, although analogies have been observed with similar systems that are thermally activated. Even when additional steps such as surface derivatization of hydroxyl groups[39] of silica or alumina are taken, leaching of metal carbonyls into solution eventually occurs. We have shown that the proper choice of solvent can prevent such leaching.

Acknowledgment. Acknowledgement is made to the donors of the Petroleum Research Fund, administered by the American Chemical Society, for partial support of this research. We also thank the University of Connecticut Research Foundation for partial support for this work.

Registry No. $Fe(CO)_5$, 13463-40-6; 1-pentene, 109-67-1; *cis*-2-pentene, 627-20-3; *trans*-2-pentene, 646-04-8; benzene, 71-43-2; isooctane, 540-84-1.

Contribution from the Department of Chemistry and Institute of Materials Science, The University of Connecticut, Storrs, Connecticut 06268

Uranyl Clay Photocatalysts

STEVEN L. SUIB* and KATHLEEN A. CARRADO

Received April 18, 1984

Uranyl-exchanged clay photocatalysts have been used to photooxidize alcohols to ketones. Luminescence excitation, emission, and lifetime studies have been used to characterize these materials before, during, and after reaction. The absorption maxima for most of the uranyl-exchanged clays shift to higher wavelengths with respect to those for other aluminosilicate catalysts. Lifetime results indicate that several sites exist on these catalysts. Saturation of alcohol/clay slurries with oxygen leads to increasing rates of ketone formation. These uranyl-sensitized photoautoxidation reactions also produce coupled products as well as aldehydes, such as acetaldehyde, as identified by gas chromatography/mass spectrometry techniques. Different clays yield different amounts of product and rates of product formation. Hectorite exchanged with uranyl ions is the most active catalyst of all aluminosilicate materials we have studied over short photolysis times.

Introduction

We have recently reported[1,2] that uranyl-exchanged zeolites are good photooxidation catalysts for isopropyl alcohol conversion to acetone. The pore size and the state of dehydration of the zeolite are important factors in this reaction. The rate of formation of acetone remained essentially the same even after 300 h of photolysis. There are two major problems, however, with these zeolite photocatalysts. One problem concerns the low yield of the products. The other problem involves the wavelength for absorption. The zeolite photooxidation catalysts absorb at 425 nm, which is an attractive wavelength for solar irradiation, but it would be useful to have systems that absorb at higher wavelengths.

Clays, like zeolites, are aluminosilicates. Clays, however, have layered structures.[3] Relatively few photochemical studies of clays have been reported. Europium- and terbium-exchanged clays have been studied with lifetime methods[4] to understand the environment of rare-earth ions in these clays. Water splitting with $Ru(bpy)_3^{2+}$ ions exchanged into clays has also been studied.[5] Fluorescent organic probes have also been used to study surface interactions.[6]

The present study involves the incorporation of uranyl ions into hectorite, montmorillonite, bentonite, and vermiculite. The luminescence excitation and emission characteristics of these materials have been studied in order to understand the behavior of uranyl ions in clays under various thermal treatments. Lifetime experiments were carried out to obtain information regarding the number of uranyl sites in these clay materials. Each of the uranyl clays was tested in photooxidation reactions of alcohols. Various products were obtained, and the reactions were shown to be catalytic. The results obtained with the clay catalysts are compared to those with zeolite catalysts.

Experimental Section

Materials. Hectorite was obtained as a white, centrifuged powder from Baroid Sales, Houston, TX. The composition of dehydrated hectorite is $Ex_xMg_{6-x}Li_xSi_8O_{20}(OH,F)_4$. Cheto clay, a natural montmorillonite, was obtained from Filtrol Corp., Chambers, AZ. Samples were ground in a mortar and pestle. The approxmate formula of cheto was $Ca_{0.24}Na_{0.07}K_{0.07}Mg_{0.32}Fe_{0.07}Al_{1.38}Si_4O_{10}(OH)_2$. The samples of vermiculite used were similar to normal packing material. The composition of dehydrated vermiculite is $Ex_xMg_3Al_xSi_{4-x}O_{10}(OH)_2$. The samples were ground in a mortar and pestle.

Bentonite, a sodium montmorillonite, was obtained in two different mesh sizes from the American Colloid Co., Skokie, IL. The samples were SPV 200 (74 μm) Microfine, HPM-20, and SPV 325 (44 μm) Volclay, Asphalt Emulsion grade powder. The composition of bentonite was $NaCa_{0.33}(Al_{1.0}Fe_{1.67}Mg_{0.33})Si_4O_{10}(OH)_2$.

Uranyl acetate dihydrate was purchased from Fisher Scientific Co., Eimer and Amend, New York, NY, lot no. 47660. Spectral grade isopropyl alcohol and acetonitrile were purchased from J. T. Baker Chemical Co., Phillipsburg, NJ.

For more details of the clay samples please refer to Table VI. Chemical analyses before and after UO_2^{2+} exchange, surface areas, and cation-exchange capacities are reported.

Synthesis of Uranyl-Exchanged Clays. Solutions of 0.10 M UO_2^{2+} were made by dissolving 4.26 g of $UO_2(CH_3CO)_2 \cdot 2H_2O$ in 100 mL of distilled and deionized water (DDW). This was added to 1.00 g of clay in a round-bottom flask and magnetically stirred for 24 h. The exchanged clays were then filtered through ground-glass funnels of fine porosity, washed with 5–10 mL of DDW, and allowed to dry in air. Most clays were ground in a mortar and pestle after drying.

Bulk Photolysis Conditions. The quartz barrel photolysis cell used in this study was 20 mm in diameter and 50 mm in length. The entry port (5-mm diameter) was stoppered during photolyses. In all cases 0.30 g of uranyl-exchanged clay was placed in the cell with 5.00 mL of a 0.65 M isopropyl alcohol in acetonitrile solution. Independent volume measurements of the solutions before and after irradiation indicated no evaporation loss in this cell. The large dimension of the cell was designed

* To whom correspondence should be addressed at the Department of Chemistry.

(1) Suib, S. L.; Bordeianu, O. G.; McMahon, K. C.; Psaras, D. 1982. In "Inorganic Reactions in Organized Media"; Holt, S. L. Ed.; American Chemical Society: Washington, DC, 1982; ACS Symp. Ser. No. 177, pp 225–238.
(2) Suib, S. L.; Kostapapas, A.; Psaras, D. *J. Am. Chem. Soc.* **1984**, *106*, 1614–1620.
(3) Pinnavaia, T. J. *Science (Washington, D.C.)* **1983**, *No. 4595*, 365–471.
(4) Bergaya, F.; Van Damme, H. *J. Chem. Soc. Faraday Trans. 2* **1983**, *79*, 505–518.
(5) (a) Nijs, H.; Cruz, M. I.; Fripiat, J. J.; Van Damme, H. *Nouv. J. Chim.* **1983**, *6*, 551–557. (b) Nijs, H.; Fripiat, J. J.; Van Damme, H. *J. Phys. Chem.* **1983**, *87*, 1279–1282. (c) Krenske, D.; Abdo, S.; Van Damme, H.; Cruz, M.; Fripiat, J. J. *J. Phys. Chem.* **1980**, *84*, 2447–2457. (d) Abdo, S.; Canesson, P.; Cruz, M.; Fripiat, J. J.; Van Damme, H. *J. Phys. Chem.* **1981**, *85*, 797–809. (e) Nijs, H.; Cruz, M.; Fripiat, J.; Van Damme, H. *J. Chem. Soc., Chem. Commun.* **1981**, 1026–1027. (f) Dellaguardla, R. A.; Thomas, J. K. *J. Phys. Chem.* **1983**, *87*, 990–998. (g) Kurimara, Y.; Nagashima, M.; Takato, K.; Tsuchida, E.; Kaneko, M.; Yamada, A. *J. Phys. Chem.* **1982**, *86*, 2432–2437. (h) Habti, A.; Keravis, D.; Levitz, P.; Van Damme, H. *J. Chem. Soc., Faraday Trans. 2* **1984**, *80*, 67–83.
(6) Dellagardia, R. A.; Thomas, J. K. *J. Phys. Chem.* **1983**, *87*, 3550–3557.

0020-1669/85/1324-0863$01.50/0

Table I. Luminescence Spectra

sample	excitation[a]	emission[a]
UO_2^{2+}-vermiculite	370, 455	517, 535 (max)
UO_2^{2+}-hectorite	370, 415 (max, 475	490, 512 (max), 536, 563
UO_2^{2+}-cheto	425, 433 (max)	505, 526 (max), 550, 575
UO_2^{2+}-325 bentonite	365, 425, 445 (max)	526
UO_2^{2+}-200 bentonite	375, 435 (max)	505, 527 (max), 550
UO_2^{2+}-ZSM-5	425	505, 520 (max)

[a] Wavelength in nm.

to provide a large area of irradiation. The photolysis setup[2] was as described elsewhere with a Xe lamp power of 748 W.

Chromatographic Analyses. Gas chromatographic analyses of the photolyzed mixtures were performed on a Hewlett-Packard Model 5880A system equipped with a thermal conductivity detector set at 210 °C. Typically 1 μL of solution was injected onto the column. The injector temperature was set at 200 °C and the oven at 80 °C. The 10-ft columns used for the separation were prepared with use of 10% Carbowax 20M on 60–80 mesh Anakrom C-22 firebrick obtained from Analabs Inc., North Haven, CT. Absolute retention times were 1.88 min (acetone), 2.97 min (isopropyl alcohol), and 5.02 min (acetonitrile).

Spectroscopic Characterization. X-ray Powder Diffraction. X-ray powder diffraction analyses of the clays both before and after ion exchange were made with a DIANO-XRD 8000 X-ray powder diffractometer equipped with a Philips Electronic source. Conditions were as listed elsewhere.[2] Room-temperature measurements were made. The changes in d_{001} spacings were used to monitor the degree of uranyl incorporation.

Luminescence Measurements. Luminescence spectra were recorded on a double Czerney–Turner scanning monochromator Model 1902 Fluorolog Spex spectrofluorometer, under conditions described elsewhere.[2] All samples were loaded into thin quartz tubes and sealed off under a vacuum of 1×10^{-3} torr. Heat treatments of samples were done by placing the quartz tubes into an oven while on the vacuum line.

Luminescence lifetime measurements were made with a PRA (Photochemical Research Associates Corp. of London, Ontario, Canada) Model 3000 system except that a pulsed nitrogen laser (PRA Nitromite), Model LN-100, was used for the excitation source. A UV–vis grating monochromator (Model 33-86-79) from Bausch and Lomb, Rochester, NY, was used between the sample compartment and the photomultiplier tube (2.0-mm slit, 16-nm band-pass). The dye used to set the laser excitation wavelength was LN7-2 from PRA (1.8×10^{-3} M stilbene in methanol), which had a range from 408 to 453 nm with a maximum at 425 nm. The PRA dye laser module, Model LN-102, was set at 425 nm. Data were collected with the use of a Model 174 phosphorescence delay unit since all lifetimes were on the order of or greater than 10 μs. A Tracor Northern multichannel analyzer and a PDP-1103 computer were used for data collection, storage, and manipulation. Deconvolution and statistical analyses were done with software provided by the PRA Corp.

GC/MS. GC/MS data were collected on a Hewlett-Packard Model 5985B GC/MS with the system autotuned with perfluorotributylamine (PFTBA). The same columns that were used for the gas chromatography analyses were used in GC/MS work. The carrier gas was He at a flow rate of 30 mL/min. The oven temperature was held isothermally at 80 °C. One-microliter samples were injected for the GC/MS analysis. An abbreviated NBS library loaded onto a H-P computer was used to help determine the unknown complexes.

Results

A. Luminescence Excitation and Emission Experiments. Clays that did not contain UO_2^{2+} ions (starting materials) did not show any luminescence when excited between 400 and 500 nm. This wavelength range was the range used in all of our excitation, emission, and lifetime experiments. In other words, the starting materials do not luminesce. We also find no evidence of luminescence from Fe^{3+} ions either in the lattice or as impurities even at liquid-nitrogen temperature.

The luminescence excitation and emission data for various uranyl clay catalysts are given in Table I. Also included is an entry for a uranyl-exchanged ZSM-5 zeolite catalyst for comparison. The excitation maxima were used to collect emission spectra and vice versa. Figure 1 shows excitation and emission spectra for uranyl-exchanged ZSM-5 and one of the uranyl-exchanged bentonite samples. These results are typical examples

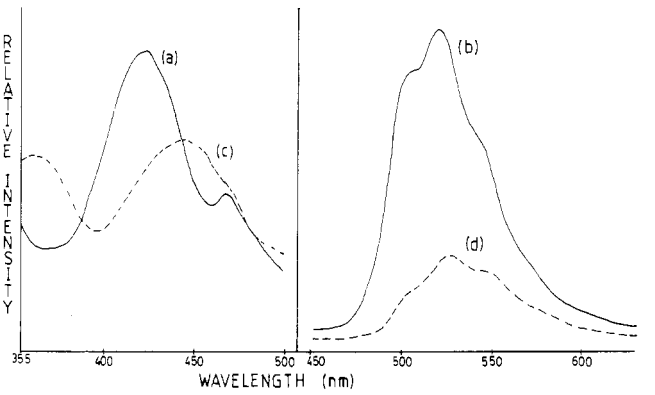

Figure 1. Luminescence spectra: (a) excitation, UO_2^{2+}–ZSM-5; (b) emission, UO_2^{2+}–ZSM-5; (c) excitation, UO_2^{2+}–bentonite; (d) emission, UO_2^{2+}–bentonite.

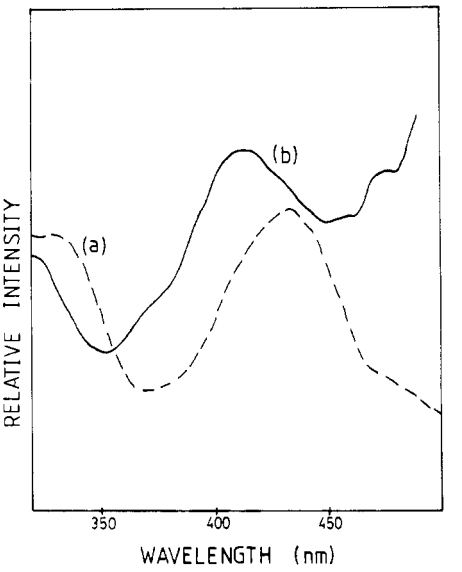

Figure 2. Excitation spectra of uranyl-exchanged (a) cheto clay and (b) hectorite clay.

Table II. X-ray Powder Diffraction Experiments

clay	$(d_{001})_{before}$[a]	$(d_{001})_{after}$[b]
hectorite	14.0	17.4
cheto	20.1	19.0
200 bentonite	14.0	17.0
325 bentonite	13.7	18.7
vermiculite	16.4	16.8

[a] The d_{001} reflection before uranyl ion exchange. [b] The d_{001} reflection after uranyl ion exchange.

of clay and zeolite photochemical behavior. Figure 2 is incorporated to show that the excitation characteristics of these clay catalysts are quite variable from one clay to another.

When the uranyl-exchanged clays are thermally treated to 370 °C, the uranyl emission bands disappear for all of the clays listed in Table I. Rehydration of these dehydrated materials does not lead to reappearance of the original uranyl emission. Less severe thermal treatment at 200 °C in some cases (i.e. bentonite), followed by rehydration, does lead to emission spectral line shapes that are similar to those of the original material. Hectorite also shows emission after 200 °C thermal treatment.

B. X-ray Powder Diffraction. Data for the d_{001} reflections for the clay catalysts before and after ion exchange of the uranyl ion are given in Table II. For comparison purposes, uranyl-exchanged ZSM-5 does not show any shifts in diffraction peaks. All samples were equilibrated with H_2O vapor for the same time period.

C. Luminescence Lifetime Data. The luminescence lifetime data for the clay catalysts are given in Table III. Unexchanged

Table III. Luminescence Lifetime Data for UO_2^{2+}–Clay or -Zeolite Systems

clay or zeolite	τ_1[a] (%)	τ_2[a] (%)	τ_3[a] (%)
cheto	23 (34)	94 (66)	none
hectorite	34 (37)	229 (63)	none
200 bentonite	6 (30)	30 (44)	81 (26)
325 benontite	5 (25)	20 (42)	69 (33)
zeolites	15–42	87–180	

[a] Lifetimes in microseconds.

Table IV. Moles of Acetone Produced on Photolysis of Uranyl–Aluminosilicate/Isopropyl Alcohol Slurries

zeolite or clay	amt of acetone,[a] 10^{-6} mol	zeolite or clay	amt of acetone,[a] 10^{-6} mol
ZSM-5	21.4	cheto	16.3
X	9.0	325 bentonite	15.7
Y	4.6	200 bentonite	18.3
hectorite	24.8	vermiculite	0.33

[a] After 30-min photolysis.

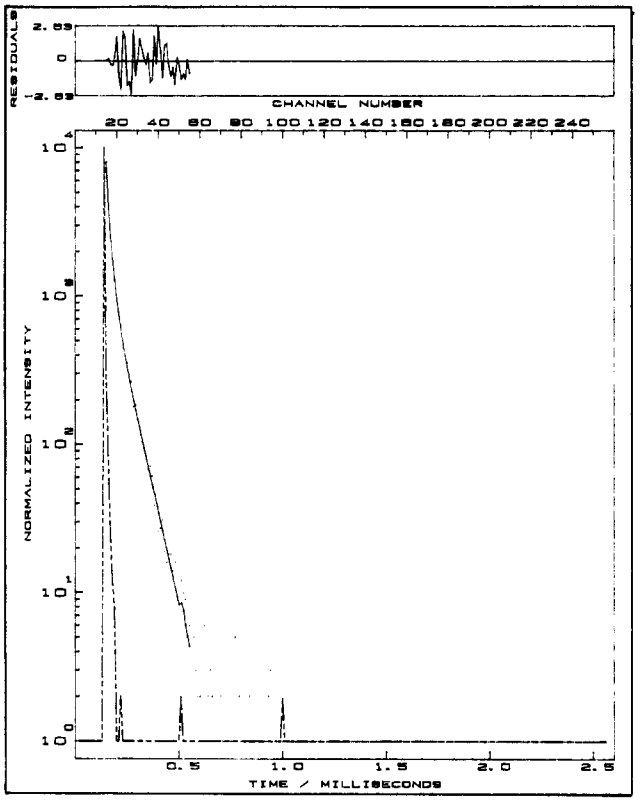

Figure 3. Luminescence lifetime decay for UO_2^{2+}–325 bentonite.

clays and purified starting clays did not show any lifetime components. A plot of the normalized intensity vs. time decay curve for UO_2^{2+}-exchanged 325 bentonite is given in Figure 3. Above the decay curve is a plot of the residuals for channels 15–55. The χ^2 value for this triple-exponential decay is 0.937. The data were fit between channels 15 and 55, inclusive.

D. Photooxidations of Isopropyl Alcohol. Each of the clay samples without uranyl ions incorporated were tested under exactly the same conditions used for isopropyl alcohol oxidation when uranyl ions were present. None of the non-uranyl-containing samples were active in the oxidation of isopropyl alcohol.

Tables IV gives the number of moles of acetone produced after 30 min of photolysis for various clays and zeolite catalysts. Long-term photolysis for a 4-h time period for the clay and zeolite catalysts is given in Figure 4. The photolysis of hectorite was carried out with and without an oxygen-saturated isopropyl alcohol/uranyl clay mixture. The results of this study are shown

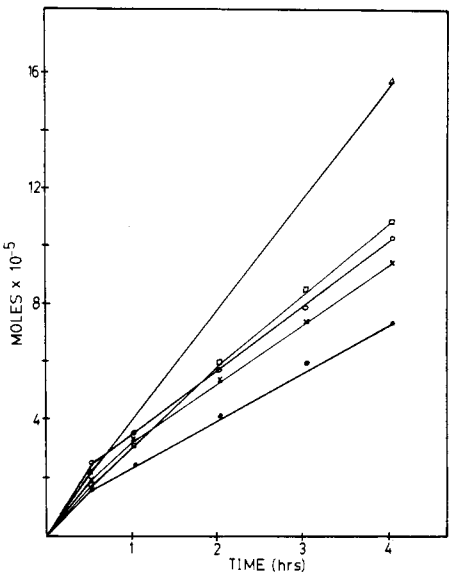

Figure 4. Moles of acetone produced on photooxidation vs. time for (△) ZSM-5, (□) cheto, (○) hectorite, (×) 200 bentonite, and (●) 325 bentonite.

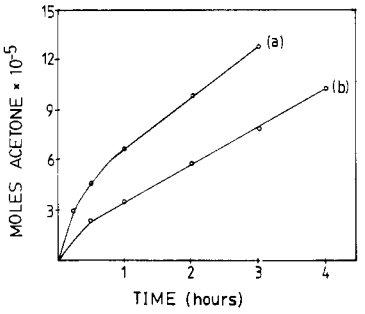

Figure 5. Oxygen promotion of acetone production in hectorite clay: (a) saturated with oxygen; (b) unsaturated with oxygen.

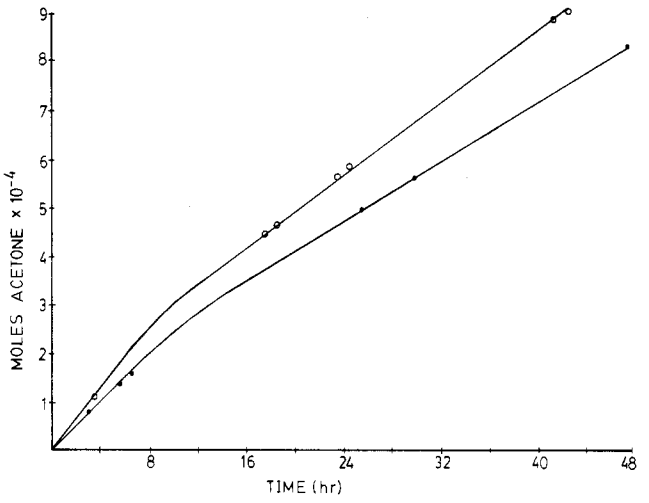

Figure 6. Deactivation study of cheto clay: (○) fresh catalyst; (●) aged catalyst.

in Figure 5. We note that in general if O_2-saturated solutions are used yields are higher. This is not so for small-pore uranyl-exchanged A and mordenite zeolite samples, which are inactive with or without oxygen-enriched solutions.

Even when oxygen is present in solution, there is some deactivation of these catalysts after prolonged irradiation. This is shown in Figure 6. The number of moles of acetone is lower for the sample that has been irradiated for a long time. For example, in Figure 6, the upper curve represents a fresh catalyst that was photolyzed for 45 h; the organic clay slurry was then washed with

Table V. GC-MS Analysis of a Cheto Clay Sample[a]

retention time, min	amt, area %	assignt
1.23	0.008	CH_3CHO
1.86	1.482[b]	CH_3COCH_3
2.19	0.033	$(CH_3)_2CHOCHO$
3.55	0.098	?

[a] 45-h photolysis. [b] 1×10^{-3} mol of acetone produced.

pure acetonitrile until no acetone was detected with gas chromatography techniques. The lower curve represents a long-term photolysis of the same cheto clay catalyst used in the upper curve. It is observed even after extensive photolysis that this catalyst is still active with similar amounts of acetone being produced.

Results with zeolite catalysts[1,2] for long-term photolysis were similar in most aspects except for one. The zeolite samples when active are selective for ketone formation. Clay samples, on the other hand, primarily produced acetone from isopropyl alcohol, but other products were observed with GC methods and identified by GC/MS techniques. Table V gives retention times, area percent, and assignments for products formed by photolysis of uranyl-exchanged cheto clay. The product that has a retention time of 3.55 min was not identified although its mass spectrum is similar to that of the isopropyl formate, which has retention time of 2.19 min. The product with the longer retention time is unknown but has significant mass fragments as high as m/e 170.

The moles of uranyl ion in each of the clays was determined by energy- and wavelength-dispersive X-ray analysis. The amounts of uranyl ion are as follows: 200 bentonite, 2.5×10^{-4} mol; 325 bentonite, 2.2×10^{-4} mol; hectorite, 2.2×10^{-4} mol; cheto, 1.8×10^{-4} mol; vermiculite, 6.8×10^{-5} mol.

Discussion

A. Luminescence Properties of Uranyl-Exchanged Clays. Even though much work has been done concerning the structure of clays and the intercalation of metal ions and complexes into clays, there have not been many reports concerning the photochemical behavior[5,6] of clays. Much recent work has concentrated on pillared clays[3] and the catalytic activity of such materials.[7-9] Clays have also been proposed as prebiological substrates,[10] as electrode materials,[11] and as asymmetric templates.[12] Several modern spectroscopic tools have been used to study clays, including EPR,[13] Auger electron spectroscopy,[12c] and NMR.[14] This short synopsis is not meant to be all inclusive but to point out major areas of recent research interests.

Two other reports that are relevant to the present work are the works of Coyne and co-workers[15] and Tsunashima, Brindley and Bastovanov.[16] The former study involves the dehydration-induced triboluminescence of kaolinite, montmorillonite, and illite clays. The latter report deals with the adsorption of uranyl ions from solution into montmorillonite.

The overall general luminescence characteristics of uranyl-exchanged zeolites and clays are very similar. The excitation and emission spectra of uranyl-exchanged ZSM-5 and bentonite of Figure 1 show the similarities and differences for two of these materials. The excitation and absorption spectra for many of the clays occur at significantly higher wavelengths than the zeolites. For instance, the maximum excitation wavelengths for vermiculite, cheto, and 325 bentonite occur at 455, 433, and 445 nm, respectively, with respect to uranyl-exchanged ZSM-5, which has a maximum excitation at 425 nm. The data of Figure 2 indicate that not all clays have red shifts to higher excitation wavelengths. These shifts in excitation maxima were not expected since uranyl-exchanged zeolites have excitation maxima that are all within 5 nm of 425 nm.

Maxima for emission spectra of the clays also shift with respect to those of zeolites. Zeolite emission maxima occur within 2 nm of 522 nm. The clay emission peak maxima range from 512 to 535 nm. Most of the clay emission spectra show significant amounts of vibrational/rotational fine structure. One exception to this is the uranyl-exchanged vermiculite clay. If analogies between uranyl zeolites[1,2] and uranyl clays can be made, then those materials with extensive vibrational/rotational fine structure are more solid in nature than solution-like.

The uranyl-exchanged hectorite samples show anomalous luminescence excitation, emission, and lifetime (vide infra) properties as compared to those of the other uranyl clay samples. This anomaly could be explained by the absence of aluminum in hectorite. The generalized molecular formulas for some of the clays used in this study are given for comparison purposes:

hectorite	$Ex_x[Mg_{6-x}Li_x]\langle Si_8\rangle O_{20}(OH,F)_4$
vermiculite	$Ex_x[Mg_3]\langle Al,Si_{4-x}\rangle O_{10}(OH)_2$
montmorillonite	$Ex_x[Al_{2-x}]\langle Si_4\rangle O_{10}(OH)_2$

In the above formulas Ex stands for exchangeable cations, the [,] symbols represent octahedral layers, and the ⟨, ⟩ symbols represent tetrahedral layers. Bentonites are specific types of montmorillonite as is cheto clay. Compositions are given in Table VI. The cation-exchange capacities (CEC) range from 85 mequiv/100 g of clay for hectorite to 140 mequiv/100 g of vermiculite.

The luminescence lifetimes of the clays as shown in Table III are at least double- and sometimes triple-exponential decays. Multiexponential decays in such systems are not always observed. Europium(III)-exchanged zeolites usually show single-exponential decay.[21] The number of lifetimes could be related to the total number of types of uranyl ion sites in the clays. The zeolite systems only have double-exponential lifetime decay patterns, indicative of two types of sites. Ion-scattering and secondary ion mass spectrometry[17] experiments suggest that these two types of sites may be external and internal uranyl ion sites. Stern–Volmer plots derived from isopropyl alcohol quenching experiments[1] also suggest two sites. Lifetimes of the clays in general fall in the same range as those of zeolites.[2] The lifetime decay shown in Figure 3 indicates that the laser profile is very narrow and therefore deconvolution from the signal should not be a problem. The randomness of the residuals and the χ^2 value mean that the fit is exceptionally good. Attempts to fit this decay to single- or double-exponential decay kinetics yielded larger χ^2 values and or nonrandom residuals.

On the other hand, a reviewer has pointed out that such multiple lifetimes could signify that the samples are mixtures. One cannot argue with this possibility, although no evidence from luminescence, emission, or X-ray data suggests that the samples are mixtures.

(7) (a) Pinnavaia, T. J.; Welty, P. K. *J. Am. Chem. Soc.* **1975**, *97*, 3819–3820. (b) Farzaneh, F.; Pinnavaia, T. J. *Inorg. Chem.* **1983**, *22*, 2216–2220. (c) Raythatha, R.; Pinnavaia, T. J. *J. Catal.* **1983**, *80*, 47–55. (d) Raythatha, R.; Pinnavaia, T. J. *J. Organomet. Chem.* **1981**, *218*, 115–122.
(8) Lahav, N.; Shani, U.; Shabtai, J. *Clays Clay Miner.* **1978**, *26*, 107.
(9) (a) Heinerman, J. J. L.; Freriks, I. L. C.; Gaaf, J.; Pott, G. T.; Collegem, J. F. G. *J. Catal.* **1983**, *80*, 145–153. (b) Gaaf, J.; Van Santen, R.; Knoester, A.; Van Wingerden, B. *J. Chem. Soc., Chem. Commun.* **1983**, 655–657.
(10) (a) Gupta, A.; Loew, G. M.; Lawless, J. *Inorg. Chem.* **1983**, *22*, 111–120. (b) Liebmann, P.; Loew, G.; Burt, S.; Lawless, J.; MacElroy, R. D. *Inorg. Chem.* **1982**, *21*, 1586–1594.
(11) Ghosh, P. K.; Bard, A. J. *J. Am. Chem. Soc.* **1983**, *105*, 5691–5693.
(12) (a) Yamagishi, A. *Inorg. Chem.* **1982**, *21*, 1778–1782. (b) Yamagishi, A. *J. Chem. Soc., Chem. Commun.* **1984**, 119–120. (c) Yamagishi, A.; Tanaka, K.; Toyoshima, I. *J. Chem. Soc., Chem. Commun.* **1982**, 343–344.
(13) (a) Schoonheydt, R. A. *J. Phys. Chem.* **1978**, *82*, 497–498. (b) Velghe, F.; Schoonheydt, R. A.; Uytterhoeven, J. B.; Peigneur, P.; Lunsford, J. H. *J. Phys. Chem.* **1977**, *81*, 1187–1194.
(14) Clayden, N. J.; Waugh, J. S. *J. Chem. Soc., Chem. Commun.* **1983**, 292–293.
(15) Coyne, L. M.; Lahav, N.; Lawless, J. G. *Nature (London)* **1981**, *292*, 819–821.
(16) Tsunashima, A.; Brindley, G. W.; Bastovanov, M. *Clays Clay Miner.* **1981**, *29*, 10–16.
(17) Suib, S. L.; Coughlin, D. F.; Otter, F. A.; Canopsk, L. *J. Catal.* **1983**, *84*, 410–422.

Table VI. Clay Characteristics

clay	composition, %	CEC[a]	surface area[b]
hectorite	SiO_2 = 58.5, Al_2O_3 = 0.2, MgO = 26.8, Na_2O = 2.6, F^- = 1.8, Li_2O = 1.2, CaO = 1.1, Fe_2O_3/FeO = 0.2, K_2O = 0.1, H_2O = 7.5	85	600
vermiculite	[c]	140	[c]
cheto	SiO_2 = 66.97, Al_2O_3 = 19.59, TiO_2 = 0.32, Fe_2O_3 = 1.52, ZrO_2 = 0.11, MnO = 0.11, MgO = 7.33, CaO = 3.77, K_2O = 0.33, Na_2O = 0.06, P_2O_5 = 0.05, SO_2 = 0.02, Cl^- = 0.05	131	[c]
200 bentonite	SiO_2 = 63.02, Al_2O_3 = 21.08, Fe_2O_3 = 3.25, FeO = 0.35, MgO = 2.67, Na_2O = 2.57, CaO = 0.65, H_2O = 5.64	70	500
325 bentonite	SiO_2 = 65.32, Al_2O_3 = 20.74, Fe_2O_3 = 3.03, FeO = 0.46, TiO_2 = 0.14, P_2O_5 = 0.01, CaO = 0.52, MgO = 2.30, Na_2O = 2.59, R_2O = 0.39, SO_3 = 0.35, H_2O = 5.14	90	500

[a] In mequiv/100 g. [b] In m^2/g; data from supplier. [c] Not available.

B. Photoassisted Catalytic Oxidations with Clays. The intercalation of uranyl ions results in an increase in the d_{001} lattice spacing for most of the clays as shown in Table II. Significant increases are observed for all these clays except for cheto clay and vermiculite. We note that the (d_{001}) values for cheto and vermiculite are already fairly large; perhaps expansion of these clays is not necessary for uranyl ion incorporation. One possibility is that the uranyl ions in the cheto clay and the vermiculite samples are only surface bound. However, bulk analyses are consistent with uranyl ion incorporation into the bulk of these clays. Vermiculite is also known not to expand even though it has a high cation-exchange capacity.[18] X-ray powder diffraction data for montmorillonite exchanged with uranyl ions[16] compare favorably (14–22 Å) with those for our samples (17–19 Å). The thermal decomposition temperature of 150 °C reported for montmorillonite[16] is similar to that of 200 °C determined by luminescence methods given here.

The short-term photooxidations of isopropyl alcohol with various clays show that uranyl-exchanged hectorite initially has the highest rate of acetone production of any material we have studied. After about 45 min of photolysis, as shown in Figure 4, uranyl-exchanged ZSM-5 becomes a better photooxidation material than all of the clays. For the most part, the uranyl-exchanged clays are more active than uranyl-exchanged zeolites. This is especially true for small-pore zeolites. The more open structure of the clays could cause these increased conversions.

Oxygen saturation of the acetonitrile/isopropyl alcohol/uranyl clay mixtures as shown in Figure 5 leads to increased amounts of acetone production. This observation suggests that uranium(VI) in the uranyl moiety is initially reduced to uranium(V). The latter species has not been isolated in zeolites or clays by luminescence, X-ray photoelectron spectroscopy, electron paramagnetic resonance, or absorption methods. The mechanism for these oxidations presumably involves reoxidation of uranium(V) to uranium(VI) by molecular oxygen.[22]

Analyses of the amount of uranyl ion in the clay samples with respect to the amount of acetone produced indicates that these reactions are catalytic. For instance, after 20 h of photolysis the ratio of moles of acetone to moles of uranyl ion in the cheto clay sample is 2.7, signifying that the reaction is catalytic. This catalyst slightly deactivates after approximately 90 h of photolysis as shown in Figure 6. The aged catalyst does show an increasing amount of acetone with a slope similar to that of the fresh catalyst.

Uranyl zeolite photolyses are selective for the production of acetone. After about 4 h of photolysis of the clays, significant amounts of other products besides acetone are formed. Acetaldehyde is common for most of the clays and can be explained by the reactions

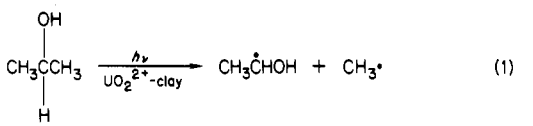

$$CH_3\overset{OH}{\overset{|}{C}}HCH_3 \xrightarrow[UO_2^{2+}\text{-clay}]{h\nu} CH_3\dot{C}HOH + CH_3\cdot \qquad (1)$$

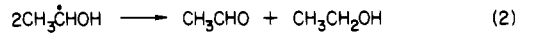

$$2CH_3\dot{C}HOH \longrightarrow CH_3CHO + CH_3CH_2OH \qquad (2)$$

From eq 1 it is observed that carbon–carbon bond cleavage competes with hydrogen abstraction, which occurs when acetone is produced. Equation 2 provides a pathway for acetaldehyde to form. Ethanol was not detected in the product analysis, and therefore hydrogen abstraction of ethanol may also occur.

The observation of isopropyl formate as a product is unusual. Obviously, some type of coupling is involved. Radical species have been isolated by EPR experiments of frozen glasses of uranyl ion/organic alcohol and acid mixtures.[19] A similar type of radical coupling probably is responsible for the unknown compound with the highest molecular weight.

Conclusions

We have shown that uranyl-exchanged clays are stable photocatalysts. The stability of these clay photocatalysts is not as high as that of similar zeolite photocatalysts. The selectivity for ketone production by uranyl clays is less than that by zeolites, but unusual coupling products can be formed. This is a general observation; photolyses of methanol, ethanol, acids, and ethers in the presence of uranyl clays lead to various radical coupling products.[20] If the aluminosilicate support is changed the excitation wavelength maxima can be significantly changed.

Acknowledgment. We wish to thank Dr. Joseph Groeger of the Institute of Materials Science for several suggestions and for determining wavelength-dispersive X-ray analyses. We also wish to thank Gary Lavigne of the IMS for help with the GC/MS work. Dr. R. Waskom of the American Colloid Co. graciously provided all bentonite starting material. The generous support of the National Science Foundation under NSF Grant No. CHE-8204417 is gratefully acknowledged.

Registry No. UO_2^{2+}, 16637-16-4; isopropyl alcohol, 67-63-0; acetone, 67-64-1.

(18) Berner, R. A. "Principles of Chemical Sedimentology"; McGraw-Hill: New York, 1971; pp 158–191.

(19) Greatorex, D.; Hill, R. J.; Kemp, T. J.; Stone, T. J. *J. Chem. Soc., Faraday Trans. 1* **1972**, *68*, 2059–2076.

(20) Suib, S. L.; Tanguay, J. F., unpublished results.

(21) Suib, S. L.; Zerger, R. D.; Stucky, G. D.; Morrison, T. I.; Shenoy, G. K. *J. Chem. Phys.* **1984**, *80*, 2203–2207.

(22) A reviewer has suggested that if reaction takes place in the interlamellar space then diffusion limitations of reactants, products, and O_2 could be important.